Macromolecules

Article

pubs.acs.org/Macromolecules

Oxidation-Responsive Poly(amino ester)s Containing Arylboronic Ester and Self-Immolative Motif: Synthesis and Degradation Study

Cheng-Cheng Song, Ran Ji, Fu-Sheng Du,* and Zi-Chen Li*

Beijing National Laboratory for Molecular Sciences, Key Laboratory of Polymer Chemistry and Physics of Ministry of Education, College of Chemistry and Molecular Engineering, Peking University, Beijing 100871, People's Republic of China

Supporting Information

ABSTRACT: We report the synthesis of a new type of amphiphilic poly(amino ester)s which can be completely degraded in aqueous media via H_2O_2 oxidation. The polymers were prepared by the controlled Michael-type addition polymerization of a phenylboronic pinacol ester-containing diacrylate and *N*-aminoethylpiperazine, followed by post-modification with mPEG5K-succinimide ester. Upon oxidation, the side chain phenylboronic esters will be transformed into phenol groups which can trigger the sequential self-immolative process to degrade the polymer main chain. Meanwhile, the amino groups on the polymer main chain are capable of trapping the highly active quinone methides generated *in situ* during the oxidative degradation of the polymers. Based on the detailed oxidation kinetics and products of several model compounds, the H_2O_2-triggered degradation of nanoparticles of these copolymers was investigated by NMR spectroscopy, GPC, and Nile red fluorescence probe. The results demonstrate that the poly(amino ester) backbones were completely degraded by H_2O_2, resulting in the dissociation of nanoparticles. Oxidative degradation rates of the nanoparticles could be accelerated by increasing the concentration of H_2O_2, the PEGylation degree, or the pH of the buffer. Interestingly, the *in situ* formed quinone methides could be captured by secondary amines due to their higher nucleophilicity than H_2O. Of potential importance, these amphiphilic oxidation-responsive copolymers are sensitive to stimulation of 200 μM H_2O_2; therefore, they may find application in the field of intelligent drug/gene delivery systems.

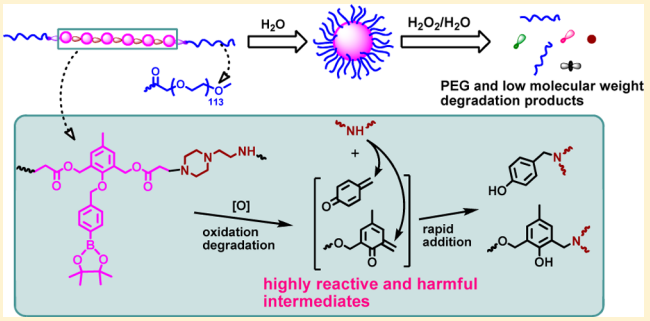

INTRODUCTION

Reactive oxygen species (ROS) at moderate concentrations play an important role in several physiological processes such as cell signaling, apoptosis, or proliferation and in the fight against foreign objects.[1] However, if ROS is overproduced, it may damage biomolecules such as lipids, proteins, and DNA. A number of evidences reveal that oxidative stress caused by overproduction of ROS is closely associated with various pathological disorders including cancer and inflammatory or neurodegenerative diseases.[2] Oxidative stress plays a pivotal role in initiation, progression, and metastasis of cancer cells; chemoresistance of some cancer cells may also be related to overproduced ROS.[3] These biological features inspired scientists to exploit various probes or sensors for the detection of different reactive oxygen species or *in vivo* diagnosis and to develop biomaterials for site-specific drug/gene delivery.[4] For example, polysulfides, poly(thioketal), selenium-containing polymers, polyoxalates, and proline-containing networks have been prepared for particulate vaccine, delivery of siRNA, DNA, or anticancer drug, *in vivo* imaging of hydrogen peroxide (H_2O_2), or as coating materials.[5]

Regarding ROS-sensitive sensors or materials, arylboronic esters have attracted great attention due to their specificity and high sensitivity to H_2O_2 that is one of the most representative ROSs *in vivo*.[4d,6] A series of small molecules used as H_2O_2-specific fluorescent probes and H_2O_2-responsive prodrugs were developed using arylboronic acid or ester as the protecting group.[4d,7] Furthermore, phenylboronic ester was also applied as a trigger to construct self-immolative dendritic fluorescent probes. Upon exposure to one molecule of H_2O_2, the dendritic probe decomposed in a domino manner and released all three fluorescent reporters, showing an amplifying effect.[8] Oxidation-responsive polymers based on phenylboronic pinacol ester were also designed and synthesized by using different synthetic routes. These polymers may find applications in the fields of polymer-based vaccine, H_2O_2-detection, *in vivo* imaging, and polymer–drug conjugates with on-demand release property.[9]

All of the aforementioned phenylboronic ester-containing compounds or polymers generate quinone methide intermediates upon H_2O_2 stimulation. Quinone methides are highly reactive electrophiles that react efficiently with biomolecules and have been reported to mediate cytotoxicity of some anticancer drugs or alkylphenol derivatives.[10,11] Although quinone methide intermediates can be quenched by water

Received: August 7, 2013
Revised: October 8, 2013
Published: October 18, 2013

Scheme 1. Synthesis of Polymers of the F Series and the PF Series[a]

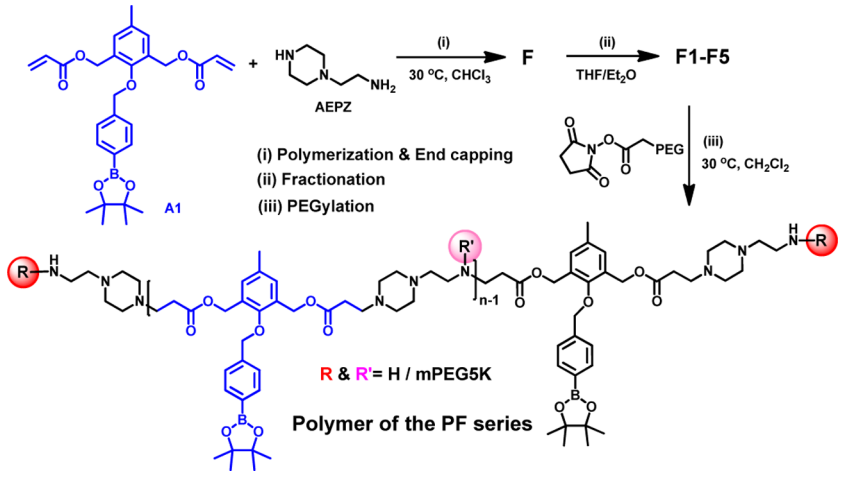

[a]The present drawing does not mean the polymers possess a head-to-tail structure.

Scheme 2. Synthesis of Monomer A1[a]

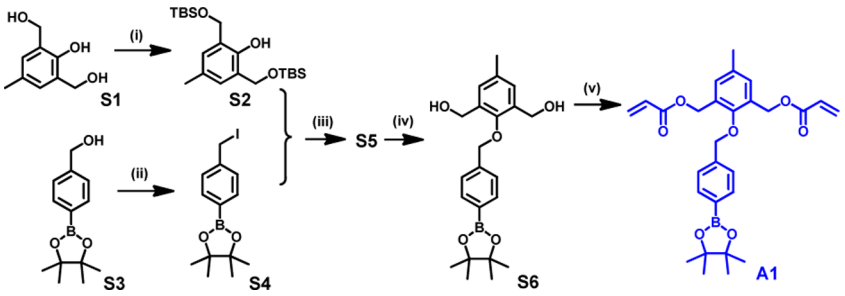

[a]Reagents and conditions: (i) TBDSCl, imidazole, DMF, 0 °C to rt, 12 h (82%); (ii) NaI, TMSCl, ACN, 0 °C to rt, 12 h (87%); (iii) DMF, K_2CO_3, 0 to 35 °C, 12 h (76%); (iv) *p*-toluenesulfonic acid, methanol, 30 °C, 2.5 h (90%); (v) acryloyl chloride, triethylamine, DCM, 0 °C to rt, 12 h (41%).

molecules to form stable and safe hydroxymethylphenol derivatives upon *in vitro* incubation in aqueous buffers, they might be harmful when the arylboronic ester-containing polymers are used *in vivo* as carrier materials.[9a,d,12] Thus, it is interesting to develop arylboronic ester-based oxidation-responsive polymers with built-in nucleophilic groups capable of catching quinone methide intermediates upon H_2O_2-triggered degradation of the polymers. In this work, phenylboronic pinacol ester-containing poly(amino ester)s with different kinds of amino groups have been prepared by Michael-type addition polymerization of the oxidation-cleavable diacrylate and *N*-aminoethylpiperazine (AEPZ) (Scheme 1). The built-in primary or secondary amino groups can be used for PEGylation to afford amphiphilic copolymers. More importantly, they are able to scavenge the *in situ* produced quinone methides upon H_2O_2 oxidation. In addition, the (co)polymers are pH-sensitive due to the presence of secondary or tertiary amino groups in the backbones. This type of oxidation-degradable, pH-sensitive (co)polymers may find applications as drug carriers for curing cancer or inflammatory diseases.

EXPERIMENTAL SECTION

Materials. 4-(4,4,5,5-Tetramethyl-1,3,2-dioxaborolan-2-yl)benzyl acrylate was synthesized as reported in the literature.[12] *N*-Aminoethylpiperazine (AEPZ, Alfa), $mOEG_4$-NH_2 (Beijing Isomersyn Technology Co.), mPEG5K-succinimide (mPEG5K-SCM, Jenkem Technology), Nile red (NR, Aldrich), and hydrogen peroxide (H_2O_2, 30 wt % Beijing Chemical Works) were used as received. Dichloromethane (DCM) and chloroform were distilled over CaH_2 after refluxing for ~6 h. Deuterated phosphate buffer with pH 7.4 was prepared from NaOD (40 wt % in D_2O, Alfa) and deuterated phosphoric acid (85 wt % in D_2O).

Synthesis of Monomer A1 and Model Molecules A2 and A3. Diacrylate monomer **A1** was synthesized according to Scheme 2. Two model molecules, **A2** and **A3**, were prepared by the Michael-type addition reaction of $mOEG_4$-NH_2 to 4-(4,4,5,5-tetramethyl- 1,3,2-dioxaborolan-2-yl)benzyl acrylate and **A1**, respectively. All of the detailed synthetic processes and characterization data are shown in the Supporting Information.

Synthesis and Fractionation of Polymer F. Monomer **A1** (503 mg, 1.02 mM) and AEPZ (132 mg, 1.02 mM) were dissolved in anhydrous chloroform (1.2 mL) in a Schlenk flask, and the reaction mixture was stirred at 30 °C under a nitrogen atmosphere. The polymerization was monitored with ^{1}H NMR and GPC. After 4 days, the polymerization was quenched by adding 80 μL of AEPZ (78.8 mg, 0.61 mM). The end-capping reaction was completed in 60 min as confirmed by ^{1}H NMR spectroscopy. The end-capped polymer **F** was obtained by precipitation from ethyl ether (Et_2O)/petroleum ether (1/1, v/v) and dried in a vacuum for 24 h at ambient temperature. Polymer **F** was further fractionated by using THF as the good solvent and Et_2O as the poor solvent at ambient temperature. Briefly, **F** (600 mg) was dissolved in 10 mL of THF, and 20 mL of Et_2O was slowly added to precipitate the highest molecular weight fraction **F1**. The supernatant was concentrated and reprecipitated in THF/Et_2O (10 mL/25 mL) mixed solvent to get fraction **F2**. By repeating the above procedure using different THF/Et_2O volume ratios, five narrowly distributed polymers were obtained (**F1**–**F5**, Table 1).

dx.doi.org/10.1021/ma401656t | *Macromolecules* 2013, 46, 8416–8425

Table 1. Molecular Weights and PDIs of Polymer F and the Five Fractions

	M_n[a]	M_p[a]	PDI[a]	yield (%)
F	11 700		3.52	95
F1	91 700	142 000	1.43	5
F2	66 100	108 000	1.48	11
F3	22 700	38 300	1.71	29
F4	12 700	20 500	1.61	18
F5	5 300	6 900	1.36	27

[a]Measured by GPC using polystyrene as standards in THF.

PEGylation of Polymers of the F Series. The PEGylated amphiphilic copolymers (**PF** series) were prepared from the **F** series precursors (**F3**−**F5**) according to Scheme 1. Using **PF4a** in Table 2 as an example, polymer **F4** (72 mg, ∼0.12 mmol of reactive amino groups) and mPEG5K-SCM (300 mg, ∼0.06 mmol) were dissolved in 3 mL of anhydrous DCM. The reaction was carried out at 30 °C for 3 days under stirring. After precipitation in Et_2O, a white powder (81% yield) was obtained. This crude polymer was further purified using preparative GPC (Japan Analytical Industry Co. Ltd., LC-9210 NEXT; $CHCl_3$ as the eluent) to remove the unconjugated PEG, affording the final polymer **PF4a**. The other PEGylated copolymers were prepared in a similar manner with the feed ratios listed in Table 2. Copolymers **PF3a** and **PF5a** were also purified using preparative GPC, while **PF4b** and **PF4c** could be simply purified by precipitation using DCM as the good solvent and Et_2O as the poor solvent.

NMR Measurements. The degradation kinetics of the monomer, model compounds, and the polymers were studied at 37 or 60 °C by monitoring the ^{1}H NMR spectra on the Bruker Avance III 400 MHz spectrometer.

Gel Permeation Chromatography (GPC). The GPC measurements were carried out on equipment consisting of a Waters 1525 binary HPLC pump, a Waters 2414 refractive index detector, and three columns (Styragel HT2, HT3, and HT4) at 35 °C with THF as the eluent (1.0 mL/min). A series of narrow dispersed polystyrenes were used for calibration. Molecular weight and polydispersity index (PDI) were calculated using the Millennium 32 software.

Oxidation of A1. Compound **A1** (2.07 mg, 4.2 μmol) was dissolved in 220 μL of acetonitrile-d_3 (ACN-d_3). After the addition of 200 μL of D_2O and thorough mixing, a ^{1}H NMR spectrum of the homogeneous solution was immediately recorded and used for the 0 time point. Then, 1 μL of H_2O_2 (30 wt %) was added to the tube to initiate the oxidation reaction at 60 °C. ^{1}H NMR spectra were collected at desired time points. Control experiment of **A1** without H_2O_2 was carried out synchronously at 60 °C.

Oxidation of Model Compounds A2 and A3. Taking the oxidation of **A2** in D_2O as an example, compound **A2** (4.0 mg in ∼0.5 mL $CDCl_3$) was charged into an NMR tube. After removing $CDCl_3$ by evaporation, 500 μL of D_2O was added to dissolve **A2** (16 mM). Upon addition of H_2O_2 (16 mM), the oxidation reaction was conducted at 37 °C and monitored *in situ* by ^{1}H NMR spectroscopy until the signals of **A2** disappeared completely. The other oxidation experiments of **A2** or **A3** in different media were carried out following the same procedure.

H_2O_2-Triggered Degradation of Copolymers of the PF Series. The oxidative degradation of polymers of the **PF** series was performed in D_2O at 37 °C. Taking **PF4a** as an example, polymer **PF4a** (3.6 mg) was fully dissolved in 250 μL of $CDCl_3$ in an NMR tube. Then, $CDCl_3$ was removed by evaporation under reduced pressure, and a thin film was formed in the tube. After 500 μL of D_2O was added, the tube was incubated at ∼4 °C for 12 h. For the oxidation experiments, 3.5 μL of H_2O_2 (1.0 wt %) was added into the tube which was incubated at 37 °C for 24 h before collecting the ^{1}H NMR spectrum. Degradation of the other polymers was conducted in a similar way. The polymer concentration was calculated based on the formula (621/492) × P_{ox} (mg/mL), where P_{ox} denotes the mass percentage of the oxidation-responsive segment in the **PF** series of polymers as listed in Table 2.

Degradation of Copolymers of the PF Series Was Also Monitored by GPC. All the polymers were degraded under the same conditions as the NMR measurements. After degradation for 1 day, the mixture was lyophilized to afford a white powder and was analyzed by GPC.

Degradation of Copolymer Nanoparticles As Followed by NR Fluorescence Probe. The dispersions of copolymers of the **PF** series were prepared following the film-rehydration procedure used for preparation of the samples in the NMR measurement. To 10 mL of the dispersion, 50 μL of NR in ethanol (1.0 mM) was added, and the mixture was equilibrated under stirring for 12 h at room temperature. The degradation of **PF4a** nanoparticles is here reported as an example. The **PF4a** dispersion (1 mL) was adjusted to pH 7.4 (100 mM) by adding 100 μL of concentrated phosphate buffer (PB, pH 7.4, 1.0 M) and incubated for 10 min at 37 °C before the fluorescence spectrum at 0 time point was collected. Then, 7.0 μL of H_2O_2 (1.0 wt %) was added, and the fluorescence spectra of the dispersion were recorded at 37 °C at desired time points. For the other degradation experiments, different phosphate buffers or varied amounts of H_2O_2 were used. The fluorescence spectra were recorded from 560 to 700 nm on a Hitachi F-4500 spectrometer with the excitation wavelength of 545 nm and a scanning rate of 240 nm/min.

RESULTS AND DISCUSSION

Synthesis and Characterization of Monomer A1 and Polymers of the F Series. The oxidation-sensitive diacrylate monomer **A1** was synthesized via the sequential steps as shown in Scheme 2. Compound **S6** was synthesized following the reported procedure.[9d] Reaction between **S6** and acryloyl chloride afforded the desired monomer **A1**, the structure of which was confirmed by NMR, FT-IR, MS spectra, and elemental analysis (Figure S2).

Michael-type addition polymerization of **A1** and **AEPZ** was carried out at 30 °C in anhydrous chloroform (Scheme 1). The polymerization was monitored by ^{1}H NMR spectroscopy and

Table 2. Characterization of the PEGylated Polymers of PF Series

F series	M_n[a]	DP (%)[b]	PEG/N[c]	PF series	M_n[d]	PDI[d]	M_n[e]	DS[e] (%)	P_{ox}[e] (%)
F3	22 700	nd[f]	1/1.8	**PF3a**	59 300	1.20	nd[f]	66	16[g]
F4	12 700	22	1/2.0	**PF4a**	48 400	1.17	80 000	57	17
			1/8.0	**PF4b**	19 500	1.30	23 700	8.7	58
			1/35	**PF4c**	13 000	1.40	17 700	3.4	78
F5	5 300	12	1/1.0	**PF5a**	45 300	1.10	70 900	93	11

[a]Molecular weight of the **F** series polymers measured by GPC using polystyrenes as standards in THF. [b]Average degree of polymerization (DP) of **F4** or **F5** calculated according to the ^{1}H NMR spectra of their PEGylated derivatives **PF4a** and **PF5a**. [c]Molar ratio of mPEG5K-SCM to the reactive (primary and secondary) amino groups in feed. [d]Molecular weight and polydispersity index of the **PF** series of copolymers measured by GPC. [e]Molecular weight (M_n), percent degree of PEG substitution (DS), and mass percentage of the oxidation-responsive segment (P_{ox}) of the **PF** series of amphiphilic copolymers calculated by the ^{1}H NMR spectra as shown in Figure 2. [f]Not calculated due to the poor resolution of the ^{1}H NMR spectrum of **PF3a**. [g]Estimated by the formula (621/(621 + 5000 × DS)) × 100%.

dx.doi.org/10.1021/ma401656t | *Macromolecules* 2013, 46, 8416−8425

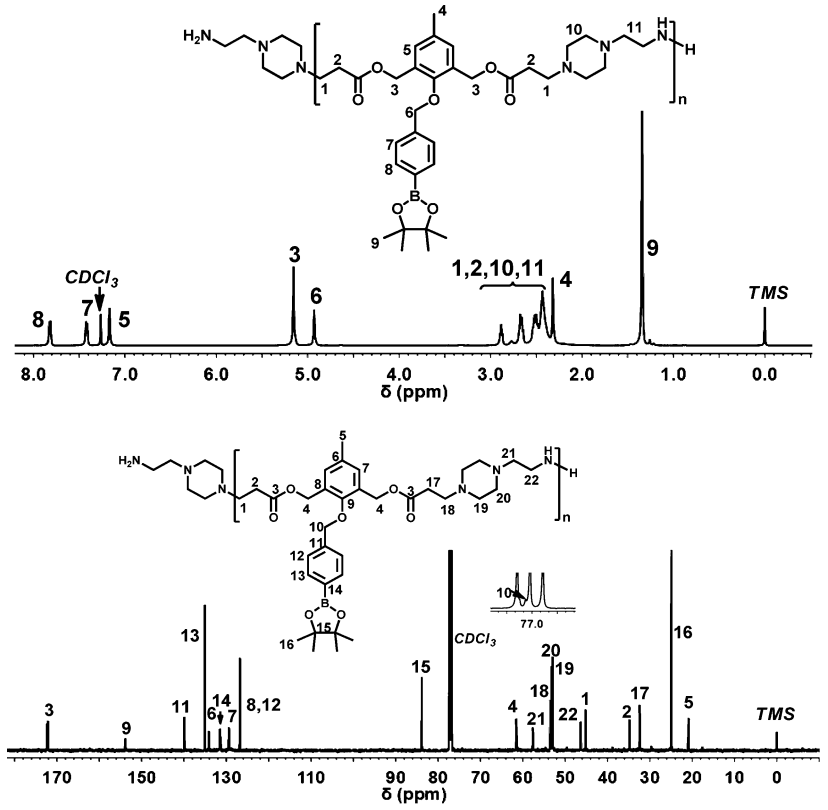

Figure 1. ^{1}H NMR and ^{13}C NMR spectra of polymer **F**.

GPC measurement (Figures S3 and S4), and the results are summarized in Table S1. After 4 days, the conversion of the acrylic double bond reached ~98%, and the M_n of the polymers reached 8900 with a PDI of 4.1. Statistically, the polymer ends may contain residual vinyl groups; therefore, we added an excess of AEPZ after the polymerization to end-cap the polymer. Since the secondary amino group of AEPZ is much more reactive than the primary one toward the Michael-type addition reaction with the acrylic double bond,[13] both ends of the capped polymer are expected to be primary amino groups. The end-capped polymer was purified by precipitation method to afford polymer **F**, the chemical structure of which was confirmed by its ^{1}H and ^{13}C NMR spectra (Figure 1).

Regarding the Michael-type addition to the acrylic double bond, the acyclic secondary amine formed by the Michael-type addition of the AEPZ primary amino group to the acrylic double bond is much less reactive than the original cyclic secondary or the primary amino groups at 40 °C in chloroform.[13] Our model reaction also revealed the linear polymer with negligible branching points was obtained at 30 °C, and the branched structure was observed only at the higher temperature, for example 60 °C (Figures S5 and S6). For polymer **F**, its ^{13}C NMR spectrum clearly demonstrated a linear structure as proven by the strong peaks at ~46 ppm (protons 1 and 22) and negligible branching signals at ~51 ppm. These results clearly indicate that polymer **F** has a linear topology with the primary amino groups at both ends and numerous secondary and tertiary amino groups in the backbone. The primary or secondary amino groups can be used for further functionalization of the polymer;[14] also, the amino groups render the polymer sensitive to pH.[15] More importantly, the primary or secondary amines can react quickly with the intermediate quinone methides produced by H_2O_2 oxidation and subsequent self-immolative elimination of polymer **F**,[10b] which is beneficial for the polymer considering its potential *in vivo* use.

Polymer **F** has a broad molecular weight distribution due to the step polymerization mechanism. We carefully fractionated **F** by using THF as the good solvent and ethyl ether as the poor solvent, and five fractions with different molecular weights and relatively low PDIs were obtained (Figure S7 and Table 1). These polymers were insoluble in water; **F3**−**F5** were used for further modification and property study.

PEGylation of Polymers of the F Series. Highly reactive water-soluble mPEG5K-SCM was used to modify **F3**−**F5** (Scheme 1). Although both primary and secondary amines in these polymers can react with *N*-hydroxysuccinimide esters, the former is much more reactive (10−1000 times) than the latter mainly due to the steric effect.[16] It is rationally speculated that the PEGylation occurs preferentially at the chain ends of the **F** series of polymers, and the degree of PEG substitution (DS) can be easily tuned by varying the feed ratio of mPEG5K-SCM to the precursor polymers. The model reactions confirmed this speculation (Figures S8 and S9). The DS of the PEGylated polymers (**PF** series) was determined by the ^{1}H NMR spectra (Figure 2).

Using the characterization of **PF4a** as an example, this polymer was obtained with a high molar feed ratio (1:2) of mPEG5K-SCM to the reactive amino groups (primary and secondary) of the precursor polymer **F4**. Therefore, it is reasonable to expect that all of the primary amino groups at the end of polymer **F4** were consumed. In the ^{1}H NMR spectrum of **PF4a**, the two peaks c (~4.0 ppm) and c′ (~4.2 ppm) are assigned to the carbonyl-adjacent methylene signals of the PEG chains conjugated to the **F4** chain ends and the polymer backbone, respectively. By comparing the integration intensities

dx.doi.org/10.1021/ma401656t | *Macromolecules* 2013, 46, 8416−8425

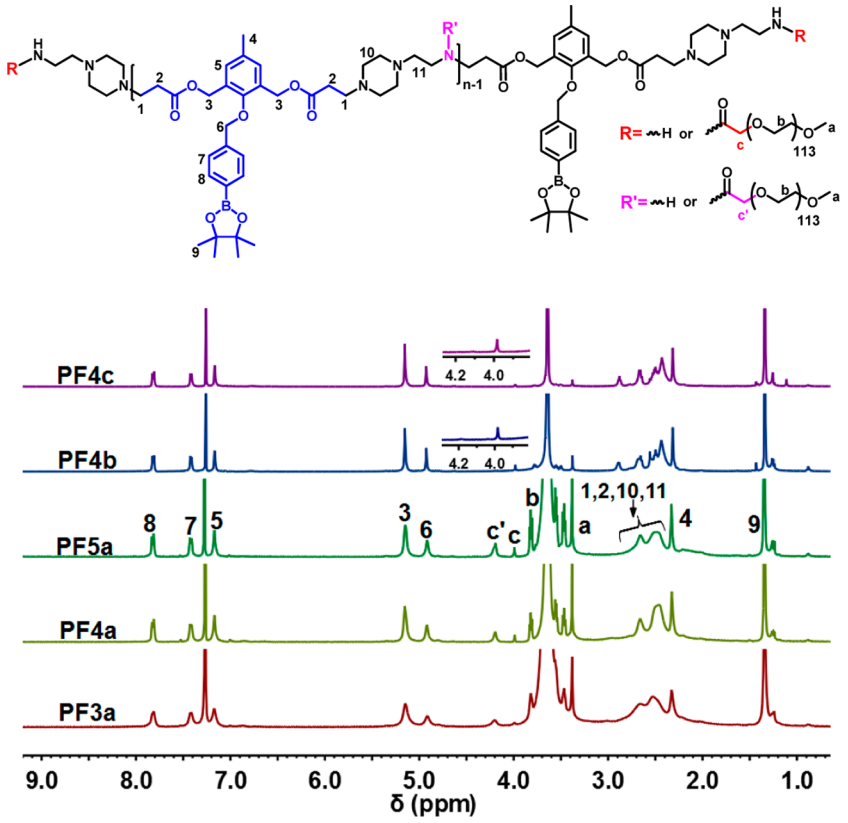

Figure 2. ^{1}H NMR spectra of the **PF** series copolymers in $CDCl_3$. Average degree of polymerization (DP) of the parent polymers **F4** and **F5** is calculated by the formula: DP = $I_6 \times 2/I_c$, where I_6 and I_c denote the integration intensity of peak c (~4.0 ppm) and peak 6 (~4.9 ppm) in the spectra of **PF4a** and **PF5a**, respectively. Percent degree of PEG substitution (DS) in the **PF** series copolymers except **PF3a** is calculated by the formula DS = $((I_c + I_{c'})/I_6) \times (DP/(DP + 1)) \times 100\%$, where $I_{c'}$ denotes the peak intensity of c′ (~4.2 ppm). For **PF3a**, DS is estimated by the formula DS = $((I_c + I_{c'})/I_6) \times 100\%$. The number-average molecular weight (M_n) of the **PF** series copolymers is calculated by the formula M_n = DP × 621 + (DP + 1) × DS × 5000. P_{ox} of the copolymers **PF4a**–**4c** and **PF5a** is calculated by the formula $P_{ox} = ((DP \times 621)/M_n) \times 100\%$.

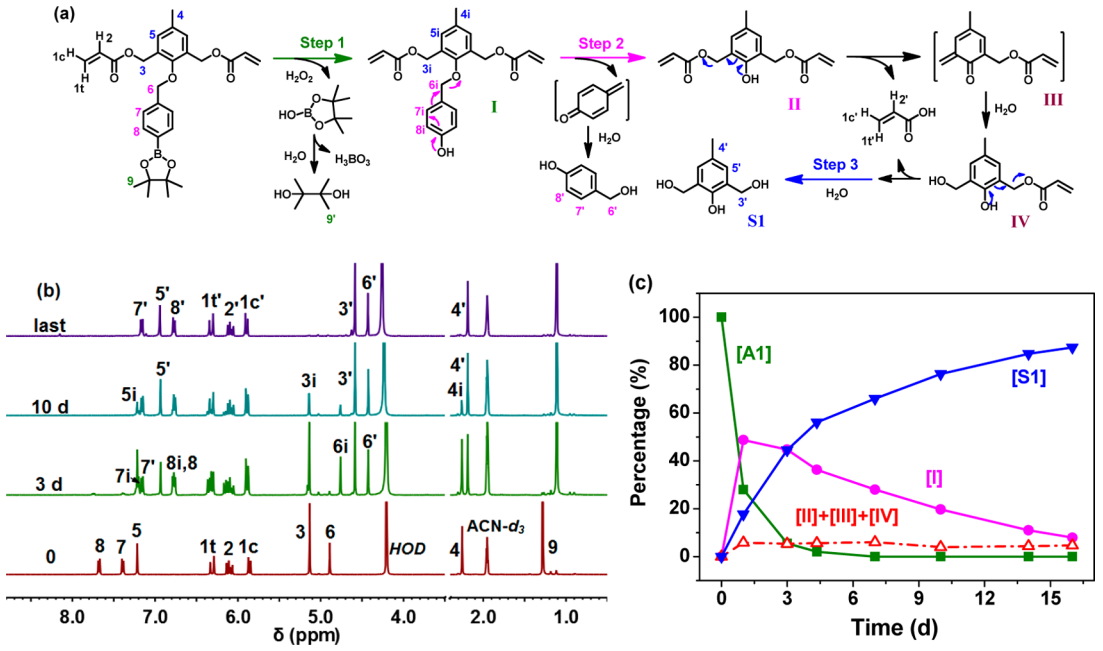

Figure 3. (a) Oxidation mechanism of **A1** triggered by H_2O_2. (b) ^{1}H NMR spectra and (c) oxidation kinetics of **A1** (5.0 mg/mL, 10 mM) in the mixed solvent of D_2O/ACN-d_3 (1/1.1, v/v) with H_2O_2 (21 mM) at 60 °C. The instantaneous percent contents of compounds **A1** and **S1** and other intermediates were calculated by the formulas: [**A1**]% = $[I_6/(I_6 + I_{6i} + I_{6'})] \times 100\%$; [**I**]% = $[I_{6i}/(I_6 + I_{6i} + I_{6'})] \times 100\%$; [**S1**]% = $[I_{3'}/(I_3 + I_{3i} + I_{3'})] \times 100\%$; ([**II**] + [**III**] + [**IV**])% = 100% − [**A1**]% − [**I**]% − [**S1**]%.

dx.doi.org/10.1021/ma401656t | *Macromolecules* 2013, 46, 8416–8425

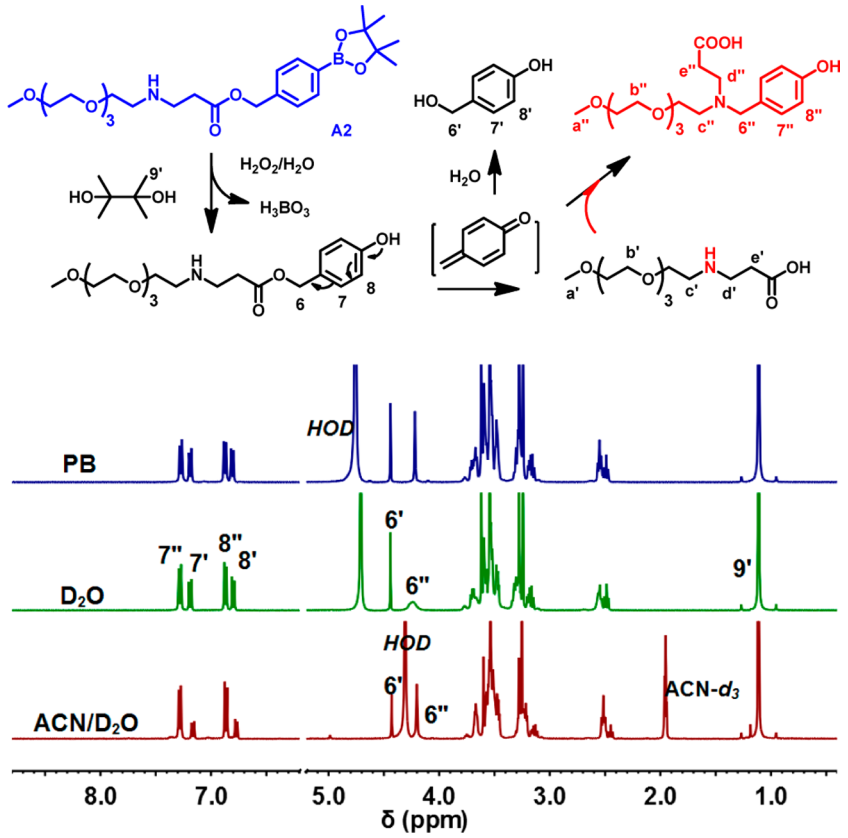

Figure 4. ^{1}H NMR spectra of **A2** (7.9 mg/mL, 16 mM) after complete oxidation by H_2O_2 (16 mM) in ACN/D_2O (1.1/1, v/v), D_2O, and PB (pH 7.4, 300 mM) at 37 °C. The trapping efficiency is calculated by the formula $(I_{7''}/(I_{7'} + I_{7''})) \times 100\%$, where $I_{7'}$ and $I_{7''}$ denote the integration intensities of peaks 7′ and 7″.

of peaks c, c′, and 6 (~4.9 ppm), the average degree of polymerization (DP) of the precursor polymer **F4** and the DS of copolymer **PF4a** were estimated to be 22 and 57%, respectively. This indicates that besides the two primary amino groups at the chain ends, ~50% of the secondary amino groups in the **F4** backbone were modified by the PEG chains. **PF4b** was obtained in a 1:8 feed ratio where only peak c, but no peak c′, was detected in the NMR spectrum; the corresponding DP was 22 and the DS was 8.7%. Therefore, only the two ends of **PF4b** have been PEGylated, and it can be considered a **PFP**-type triblock copolymer. By further decreasing the feed ratio to 1:35, **PF4c** was obtained with a DS of 3.4%, implying that one polymer chain averagely contains ~0.8 PEG. In other words, **PF4c** is a mixture of the unPEGylated **F4**, diblock, and probably triblock copolymers.

Similarly, in the ^{1}H NMR spectrum of copolymer **PF5a**, both peak c and peak c′ are clearly observable. More than 90% of the reactive amines (primary or secondary) were PEGylated because of the high feed ratio (1:1). The DS of **PF3a** was only roughly estimated (Figure 2) for copolymer **PF3a** because the ^{1}H NMR spectrum was not finely resolved due to the high molecular weight of its precursor **F3**, making it difficult to calculate the DP of **F3**. The characterization results are summarized in Table 2.

Oxidation of Monomer A1 by H_2O_2. Monomer **A1** is hydrophobic and not soluble in water. The H_2O_2-triggered oxidation of **A1** was carried out in a mixture of D_2O and ACN-d_3 at 60 °C. According to the literature,[8,9d] upon oxidation, **A1** will first be transformed to the phenolic compound **I** (Figure 3a), releasing the boronic pinacol ester which is quickly hydrolyzed to boronic acid and pinacol. Afterward, compound **I** decomposes to *p*-hydroxymethylphenol, compound **S1**, and acrylic acid via the sequential steps of 1,6- and 1,4-elimination (Figure 3a). This mechanism was confirmed by the ^{1}H NMR spectra shown in Figure 3b. The signals of the intermediate compound **I** were clearly resolved during the oxidation process.

The kinetic curves of **A1** oxidation (step 1), decomposition of compound **I** (step 2), and the formation of compound **S1** (step 3) were obtained from these spectra and are shown in Figure 3c. The rapid decomposition of monomer **A1** with a significant accumulation of compound **I** at the initial stage indicates the faster kinetics of step 1 than step 2. The amounts of the intermediates **II**, **III**, and **IV** were negligible, suggesting that the decomposition of compound **I** (step 2) is the rate-determining step in the whole process. In the absence of H_2O_2, **A1** could not be oxidized, but the pinacol unmasking reaction occurred due to the dynamic covalent chemistry (Figure S11).[17]

Oxidation of **A1** by H_2O_2 was also studied in a mixture of deuterated PB (pH 7.4, 100 mM) and ACN-d_3 at 60 °C (Figure S12). As compared with the kinetics in D_2O/ACN-d_3, **A1** was oxidized and decomposed much faster into the final products in PB/ACN-d_3. Both **A1** and compound **I** completely disappeared, and acrylic acid was generated quantitatively within 6 h. These results can be explained by the pH difference of the media. It is well-known that both the oxidation of phenylboronic ester/acid and the subsequent self-immolative eliminations are pH-dependent, undergoing a faster reaction at a relatively higher pH.[6,18] It is noted that compound **S1** has a poor solubility in PB/ACN-d_3, resulting in the relatively lower

dx.doi.org/10.1021/ma401656t | *Macromolecules* 2013, 46, 8416−8425

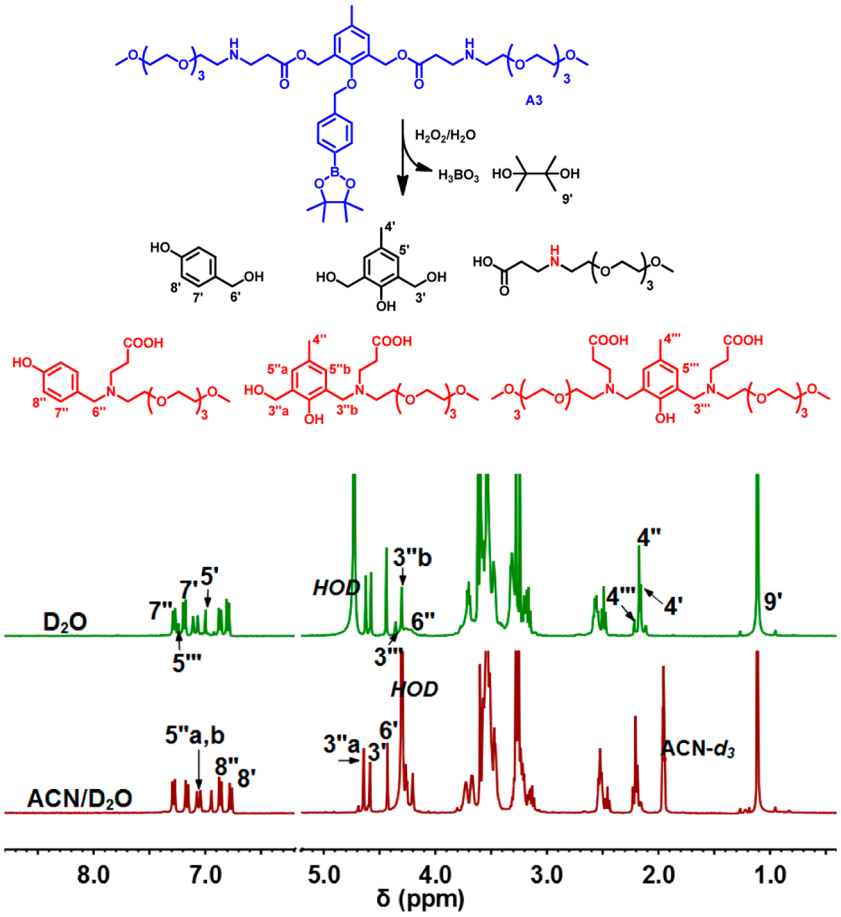

Figure 5. ^{1}H NMR spectra of **A3** (8.5 mg/mL, 9.3 mM) after completely oxidation triggered by H_2O_2 (9.3 mM) at 37 °C in ACN/D_2O and D_2O.

proton signals as compared with *p*-hydroxymethylphenol or acrylic acid. When the oxidation of **A1** was carried out at 37 °C in PB/ACN-d_3, we observed various phosphate intermediates produced by the addition of phosphate anions to the highly reactive quinone methides (Scheme S1 and Figure S13). These organophosphates gradually hydrolyzed.

Oxidation of A2 and A3. In order to clarify if the secondary amines react preferentially with the *in situ* formed quinone methides during the oxidation process, two model compounds **A2** and **A3** that are well dispersible in water were synthesized by the Michael-type addition of mOEG$_4$-NH$_2$ to the corresponding acrylate precursors (Figure S14). These two compounds were oxidized by H_2O_2 at 37 °C in different media, and the oxidation products were analyzed by ^{1}H NMR. As shown in Figure 4 for compound **A2**, the proton signals (peaks 6′, 7′, and 8′) of *p*-hydroxymethylphenol are clearly observable. Besides, the proton signals 6″, 7″, and 8″ can be assigned to the addition product of the *in situ* formed secondary amine and *p*-quinone methide. By comparing the integration intensities of peak 7″ (∼7.3 ppm) and peak 7′ (∼7.2 ppm), the trapping efficiencies of *p*-quinone methide by the amine can be calculated as 77% (ACN/D_2O), 62% (D_2O), and 57% (PB, pH 7.4), respectively. The lowest efficiency in PB was partly attributed to the competitive addition of the phosphate anion to *p*-quinone methide (Figure S15).

For the oxidation of **A3** in the presence of H_2O_2, we speculate that besides the intermediate *p*-quinone methide, the *in situ* formed *o*-quinone methides also react quickly with the secondary amino groups (Scheme S2). This is confirmed by the ^{1}H NMR spectra of **A3** oxidized by H_2O_2 (Figure 5). In both ACN/D_2O and D_2O, the proton signals (peaks 3″−5″ and 3‴−5‴) of the addition products derived from *o*-quinone methides were clearly detected (Figure S16).

Oxidative Degradation of Polymers of the PF Series. The amphiphilic copolymers of the **PF** series (**PF3a**−**5a** and **PF4b**) can self-assemble into stably dispersed nanoparticles in aqueous solution (Table S2 and Figure S18). The proton signals of the PEG chains in the nanoparticles were clearly observed in the absence of H_2O_2, but the oxidation-responsive segment was hardly detectable due to its hydrophobic feature (Figure S19). These nanoparticles were oxidized by H_2O_2 in pure water at 37 °C for 24 h, and their ^{1}H NMR spectra were recorded as shown in Figure 6. For the highly PEGylated **PF5a** with few secondary amino groups, only *p*-hydroxymethylphenol and compound **S1** are the aromatic degradation products; no other aromatic compounds derived from the quinone methides were detected. Also, the proton signals c (∼4.0 ppm) and c′ (∼4.3 ppm) of the detached PEG are clearly observable. In the case of **PF3a**, **PF4a**, and **PF4b**, the aromatic adducts of the secondary amino groups and the quinone methides were produced as indicated by the proton signals 7″, 8″, 5″, and 4″ (Figure 6 and Figure S20). With decreasing degree of PEG substitution (**PF4a** vs **PF4b**), more *in situ* formed quinone methides were captured by the unPEGylated secondary amines. When **PF4a** nanoparticles were incubated in water at 37 °C for 24 h in the absence of H_2O_2, negligible degradation products were observed (Figure S22). In PB (pH 7.4), **PF4a** can also be oxidized quickly to produce *p*-hydroxymethylphenol phosphate

dx.doi.org/10.1021/ma401656t | *Macromolecules* 2013, 46, 8416−8425

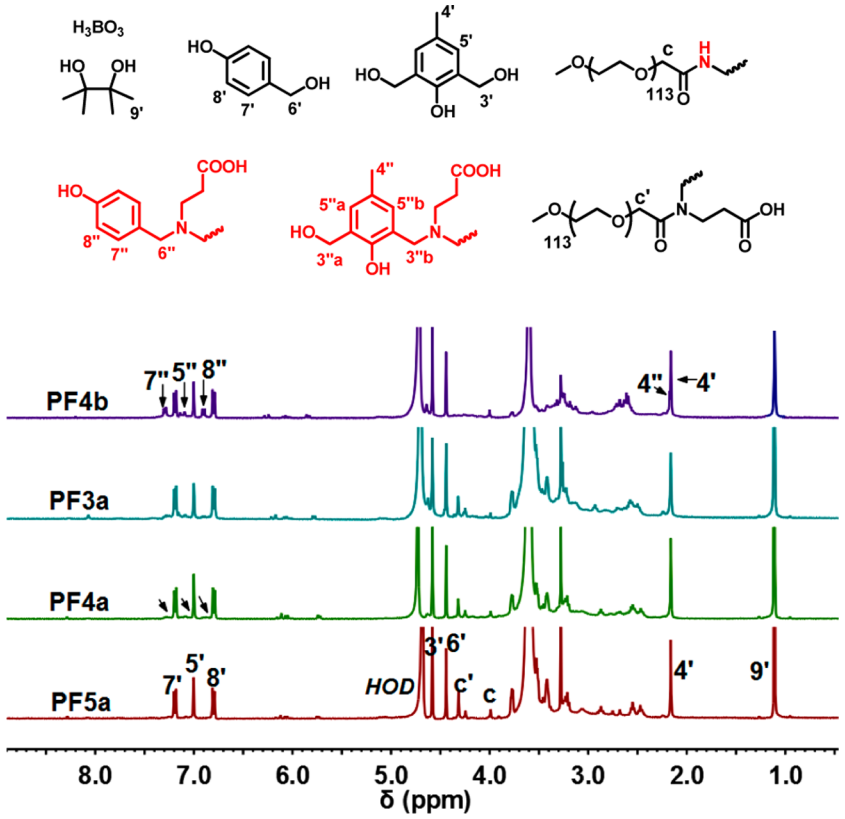

Figure 6. ^{1}H NMR spectra of **PF** series copolymer nanoparticles degraded in D_2O triggered by H_2O_2 (2 mM); 24 h, 37 °C.

that hydrolyzed gradually into *p*-hydroxymethylphenol. As mentioned in the previous section, compound **S1** is poorly soluble in the phosphate buffer, resulting in its weak proton signals (Figures S23 and S24).

The H_2O_2-triggered degradation of copolymers of the **PF** series was further confirmed by GPC (Figure 7). After oxidation in water, the original copolymers (**PF3a**–**PF5a**) completely disappeared, and only the low molecular weight mPEG5K was observed in the GPC traces. After the degradation in PB, a similar GPC trace was obtained, indicating the complete degradation of **PF4a**.

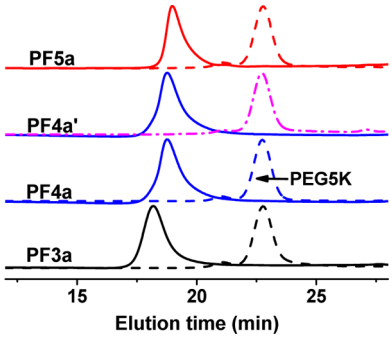

Figure 7. GPC curves of the copolymers **PF3a**–**PF5a** before (solid line) and after (dashed line) degradation in water. The dash-dotted line (**PF4a**′) denotes the degraded sample of **PF4a** in PB (pH 7.4, 300 mM). H_2O_2 concentration: 2.0 mM, 37 °C, 24 h.

pH-Dependent Degradation of Copolymer Nanoparticles of the PF Series As Studied by NR Fluorescence Probe. NR is a solvatochromic dye with strong fluorescence in a hydrophobic microdomain, but its quantum yield is drastically reduced in aqueous buffer.[19] NR was used as a fluorescence probe to study the dissociation of various pH-sensitive nanoparticles.[12,20] In this work, the degradation profiles of the **PF** nanoparticles were also studied at 37 °C using NR as a probe. As shown in Figure 8a, the fluorescence intensity of NR remained constant in the absence of H_2O_2 at pH 7.4, indicating no obvious degradation of the **PF4a** nanoparticles in the tested period. Addition of H_2O_2 caused a drastic decrease in NR fluorescence; the decreasing magnitude was greatly dependent on the H_2O_2 concentration. The intensity of NR fluorescence decreased ~30% of its initial value in the presence of 0.2 mM H_2O_2, that is approximately one-tenth of the arylboronic ester units in the polymer, indicating the partial degradation of the nanoparticles. With increasing H_2O_2 concentration to 2.0 mM, the intensity dropped rapidly to <10% of the initial value. Further increasing H_2O_2 concentration to 5.0 mM did not obviously accelerate the degradation kinetics. These results demonstrate that **PF4a** nanoparticles are sufficiently sensitive to bio-related oxidation environments.[9a]

The pH-dependent degradation results of **PF4a** nanoparticles monitored by NR are shown in Figure 8b. As expected, in the absence of H_2O_2, the normalized intensity gradually decreased with decreasing pH because of the protonation of the amino groups and the consequential swelling or partial dissociation of the nanoparticles at lower pH. When 2.0 mM H_2O_2 was added, the intensity quickly decreased to ~8% of the initial value, indicating rapid degradation of the nanoparticles. Interestingly, the degradation rate was slightly slower at pH 5.2 than at pH 7.4 or 6.5, which can be ascribed to the combined result of protonation of the amines and oxidation triggered cleavage of the polymer backbone. A lower pH is beneficial for the protonation of

dx.doi.org/10.1021/ma401656t | *Macromolecules* 2013, 46, 8416–8425

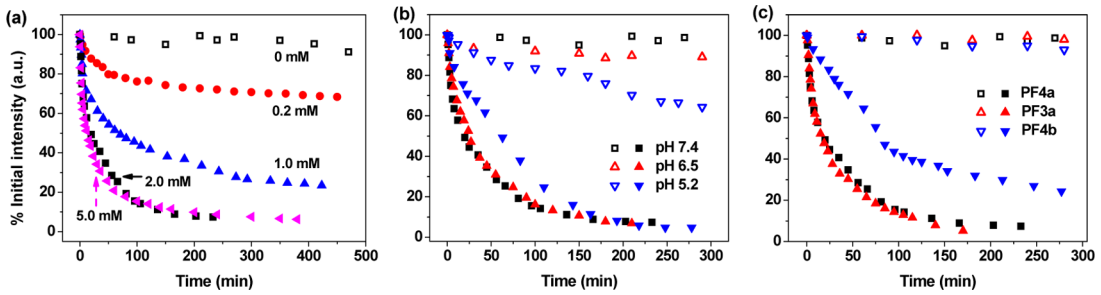

Figure 8. Time-dependent change in the normalized intensity of NR fluorescence in **PF4a** nanoparticles (a) at different H_2O_2 concentrations and (b) at different pHs without (empty) or with (solid) H_2O_2 (2.0 mM), and (c) in **PF3a**, **PF4a**, and **PF4b** nanoparticles without (empty) or with (solid) H_2O_2 (2.0 mM). NR concentration: 5×10^{-6} mol/L; 37 °C; pH 7.4.

amines but slows down the phenylboronic ester oxidation and the subsequent self-immolative elimination.

Figure 8c shows the degradation kinetics of **PF3a**, **PF4a**, and **PF4b** nanoparticles in PB. **PF3a** and **PF4a** nanoparticles exhibited similar degradation profiles, while **PF4b** nanoparticles degraded at a much slower rate. These results might demonstrate that the degree of PEGylation, not the molecular weight of the polymer precursors (**F3** vs **F4**), mainly influenced the degradation kinetics of the copolymer nanoparticles. Compared with **PF3a or PF4a** nanoparticles, the oxidation-responsive segments in **PF4b** nanoparticles are located in the more hydrophobic microdomains that have a lower permeability to H_2O_2 as well as water molecules.[21] H_2O_2-induced oxidative degradation of the **PF4b** nanoparticles was further confirmed by the light scattering and TEM measurements (Figure S25).

CONCLUSION

By combining Michael-type addition polymerization and postmodification, a series of PEGylated poly(amino ester)s containing phenylboronic ester were synthesized. These oxidation/pH dual responsive amphiphilic copolymers can self-assemble in aqueous media into nanoparticles that degrade upon oxidation by H_2O_2. Based on the oxidation results of model compounds, the degradation kinetics and products of the copolymer nanoparticles were investigated. Increasing the concentration of H_2O_2, the pH of the media, and the PEGylation degree of the copolymers accelerated the degradation. More importantly, the quinone methides generated *in situ* during the degradation of the polymers could be captured by the built-in secondary amino groups. Such a feature may improve biocompatibility of the degradation products when these polymer nanoparticles are considered for potential *in vivo* application.

ASSOCIATED CONTENT

Supporting Information

Detailed synthetic procedures, ^{1}H and ^{13}C NMR spectra and FT-IR spectrum of **A1**, **A2**, and **A3**; NMR spectra of the model molecules, GPC curves of polymers, more ^{1}H NMR spectra of the oxidation products. This material is available free of charge via the Internet at http://pubs.acs.org.

AUTHOR INFORMATION

Corresponding Authors

*Phone +86-10-62757155; Fax +86-10-62751708; e-mail fsdu@pku.edu.cn (F.D.).

*Phone +86-10-62755543; Fax +86-10-62751708; e-mail zcli@pku.edu.cn (Z.L.).

Notes

The authors declare no competing financial interest.

ACKNOWLEDGMENTS

This work was financially supported by the National Natural Science Foundation of China (21174002 and 21090351) and the National Science Fund for Distinguished Young Scholars of China (21225416).

REFERENCES

(1) (a) Oktyabrsky, O.; Smirnova, G. *Biochemistry (Moscow)* **2007**, *72*, 132−145. (b) Khutoryanskiy, V. V.; Tirelli, N. *Pure Appl. Chem.* **2008**, *80*, 1703−1718. (c) Niethammer, P.; Grabher, C.; Look, A. T.; Mitchison, T. J. *Nature* **2009**, *459*, 996−1000.

(2) (a) Coussens, L. M.; Werb, Z. *Nature* **2002**, *420*, 860−867. (b) Winterbourn, C. C. *Nat. Chem. Biol.* **2008**, *4*, 278−286. (c) Maloy, K. J.; Powrie, F. *Nature* **2011**, *474*, 298−306. (d) Zhou, R.; Yazdi, A. S.; Menu, P.; Tschopp, J. *Nature* **2011**, *469*, 221−225. (e) Gupta, S. C.; Hevia, D.; Patchva, S.; Park, B.; Koh, W.; Aggarwal, B. B. *Antioxid. Redox Signaling* **2012**, *16*, 1295−1322.

(3) (a) Trachootham, D.; Alexandre, J.; Huang, P. *Nat. Rev. Drug Delivery* **2009**, *8*, 579−591. (b) Smith, D. G.; Magwere, T.; Burchill, S. A. *Expert Rev. Anticancer Ther.* **2011**, *11*, 229−249.

(4) (a) Lee, S. H.; Gupta, M. K.; Bang, J. B.; Bae, H.; Sung, H. J. *Adv. Healthcare Mater.* **2013**, *2*, 908−915. (b) Vo, C. D.; Kilcher, G.; Tirelli, N. *Macromol. Rapid Commun.* **2009**, *30*, 299−315. (c) Lallana, E.; Tirelli, N. *Macromol. Chem. Phys.* **2013**, *214*, 143−158. (d) Lippert, A. R.; Van de Bittner, G. C.; Chang, C. J. *Acc. Chem. Res.* **2011**, *44*, 793−804. (e) Schäferling, M.; Grögel, D. B.; Schreml, S. *Microchim. Acta* **2011**, *174*, 1−18. (f) Zhou, J.; Tsai, Y.-T.; Weng, H.; Tang, L. *Free Radical Biol. Med.* **2012**, *52*, 218−226.

(5) (a) Napoli, A.; Valentini, M.; Tirelli, N.; Müller, M.; Hubbell, J. A. *Nat. Mater.* **2004**, *3*, 183−189. (b) Rehor, A.; Schmoekel, H.; Tirelli, N.; Hubbell, J. A. *Biomaterials* **2008**, *29*, 1958−1966. (c) Allen, B. L.; Johnson, J. D.; Walker, J. P. *ACS Nano* **2011**, *5*, 5263−5272. (d) Wilson, D. S.; Dalmasso, G.; Wang, L.; Sitaraman, S. V.; Merlin, D.; Murthy, N. *Nat. Mater.* **2010**, *9*, 923−928. (e) Shim, M. S.; Xia, Y. *Angew. Chem., Int. Ed.* **2013**, *52*, 6926−6929. (f) Ma, N.; Li, Y.; Xu, H.; Wang, Z.; Zhang, X. *J. Am. Chem. Soc.* **2010**, *132*, 442−443. (g) Liu, J.; Pang, Y.; Zhu, Z.; Wang, D.; Li, C.; Huang, W.; Zhu, X.; Yan, D. *Biomacromolecules* **2013**, *14*, 1627−1636. (h) Lee, D.; Khaja, S.; Velasquez-Castano, J. C.; Dasari, M.; Sun, C.; Petros, J.; Taylor, W. R.; Murthy, N. *Nat. Mater.* **2007**, *6*, 765−769. (i) Lee, Y.-D.; Lim, C.-K.; Singh, A.; Koh, J.; Kim, J.; Kwon, I. C.; Kim, S. *ACS Nano* **2012**, *6*, 6759−6766. (j) Yu, S. S.; Koblin, R. L.; Zachman, A. L.; Perrien, D. S.; Hofmeister, L. H.; Giorgio, T. D.; Sung, H.-J. *Biomacromolecules* **2011**, *12*, 4375−4366.

(6) Kuivila, H. G. *J. Am. Chem. Soc.* **1954**, *76*, 870−874.

(7) (a) Van de Bittner, G. C.; Bertozzi, C. R.; Chang, C. J. *J. Am. Chem. Soc.* **2013**, *135*, 1783−1795. (b) Karton-Lifshin, N.; Segal, E.;

Omer, L.; Portnoy, M.; Satchi-Fainaro, R.; Shabat, D. *J. Am. Chem. Soc.* **2011**, *133*, 10960−10965. (c) Major Jourden, J. L.; Cohen, S. M. *Angew. Chem., Int. Ed.* **2010**, *49*, 6795−6797. (d) Kuang, Y.; Balakrishnan, K.; Gandhi, V.; Peng, X. *J. Am. Chem. Soc.* **2011**, *133*, 19278−19281. (e) Hagen, H.; Marzenell, P.; Jentzsch, E.; Wenz, F.; Veldwijk, M. R.; Mokhir, A. *J. Med. Chem.* **2012**, *55*, 924−934.

(8) Sella, E.; Shabat, D. *Chem. Commun.* **2008**, 5701−5703.

(9) (a) Broaders, K. E.; Grandhe, S.; Fréchet, J. M. *J. Am. Chem. Soc.* **2011**, *133*, 756−758. (b) Li, C.; Hu, J.; Liu, T.; Liu, S. *Macromolecules* **2011**, *44*, 429−431. (c) Li, C.; Wu, T.; Hong, C.; Zhang, G.; Liu, S. *Angew. Chem., Int. Ed.* **2012**, *51*, 455−459. (d) de Gracia Lux, C.; Joshi-Barr, S.; Nguyen, T.; Mahmoud, E.; Schopf, E.; Fomina, N.; Almutairi, A. *J. Am. Chem. Soc.* **2012**, *134*, 15758−15764. (e) Viger, M. L.; Sankaranarayanan, J.; de Gracia Lux, C.; Chan, M.; Almutairi, A. *J. Am. Chem. Soc.* **2013**, *135*, 7847−7850. (f) Zhang, Y.; Yin, Q.; Yin, L.; Ma, L.; Tang, L.; Cheng, J. *Angew. Chem., Int. Ed.* **2013**, *52*, 6435−6439.

(10) (a) Weinstain, R.; Baran, P. S.; Shabat, D. *Bioconjugate Chem.* **2009**, *20*, 1783−1791. (b) Bentley, T. W. *Org. Biomol. Chem.* **2011**, *9*, 6685−6690. (c) Modica, E.; Zanaletti, R.; Freccero, M.; Mella, M. *J. Org. Chem.* **2001**, *66*, 41−52. (d) Pande, P.; Shearer, J.; Yang, J.; Greenberg, W. A.; Rokita, S. E. *J. Am. Chem. Soc.* **1999**, *121*, 6773−6779.

(11) (a) Thompson, D. C.; Perera, K.; London, R. *Chem. Res. Toxicol.* **1995**, *8*, 55−60. (b) Wang, P.; Song, Y.; Zhang, L.; He, H.; Zhou, X. *Curr. Med. Chem.* **2005**, *12*, 2893−2913. (c) Richter, S. N.; Maggi, S.; Mels, S. C.; Palumbo, M.; Freccero, M. *J. Am. Chem. Soc.* **2004**, *126*, 13973−13979. (d) Cao, S.; Wang, Y.; Peng, X. *Chem.—Eur. J.* **2012**, *18*, 3850−3854.

(12) Song, C.-C.; Ji, R.; Du, F.-S.; Liang, D.-H.; Li, Z.-C. *ACS Macro Lett.* **2013**, *2*, 273−277.

(13) Wu, D.; Liu, Y.; He, C.; Chung, T.; Goh, S. *Macromolecules* **2004**, *37*, 6763−6770.

(14) (a) Wu, D.-C.; Liu, Y.; He, C.-B. *Macromolecules* **2008**, *41*, 18−20. (b) You, Y.-Z.; Hong, C.-Y.; Pan, C.-Y. *Macromolecules* **2009**, *42*, 573−575.

(15) Lynn, D. M.; Amiji, M. M.; Langer, R. *Angew. Chem., Int. Ed.* **2001**, *40*, 1707−1710.

(16) Cline, G. W.; Hanna, S. B. *J. Am. Chem. Soc.* **1987**, *109*, 3087−3091.

(17) Bowie, R.; Musgrave, O. *J. Chem. Soc.* **1963**, 3945−3949.

(18) Amir, R. J.; Pessah, N.; Shamis, M.; Shabat, D. *Angew. Chem., Int. Ed.* **2003**, *42*, 4494−4499.

(19) (a) Dutta, A. K.; Kamada, K.; Ohta, K. *J. Photochem. Photobiol. A: Chem.* **1996**, *93*, 57−64. (b) Kucherak, O. A.; Oncul, S.; Darwich, Z.; Yushchenko, D. A.; Arntz, Y.; Didier, P.; Mély, Y.; Klymchenko, A. S. *J. Am. Chem. Soc.* **2010**, *132*, 4907−4916.

(20) (a) Song, C.-C.; Su, C.-C.; Cheng, J.; Du, F.-S.; Liang, D.-H.; Li, Z.-C. *Macromolecules* **2013**, *46*, 1093−1100. (b) Gillies, E. R.; Jonsson, T. B.; Fréchet, J. M. *J. Am. Chem. Soc.* **2004**, *126*, 11936−11943.

(21) Qiao, Z.-Y.; Du, F.-S.; Zhang, R.; Liang, D.-H.; Li, Z.-C. *Macromolecules* **2010**, *43*, 6485−6494.